

Synthesis of Polyacetylenes Having Pendant Carbazole Groups and Their Photo- and Electroluminescence Properties

Fumio Sanda,^{*,†} Takafumi Nakai,[†] Norihisa Kobayashi,[‡] and Toshio Masuda^{*,†}

Department of Polymer Chemistry, Graduate School of Engineering, Kyoto University, Kyoto 615-8510, Japan and Department of Information and Image Sciences, Chiba University, Chiba 263-8522, Japan

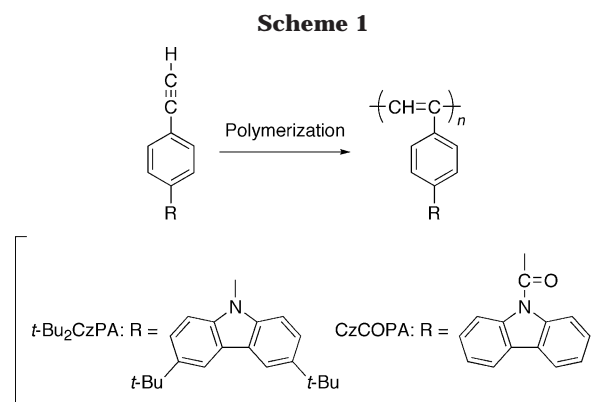
Received December 22, 2003; Revised Manuscript Received February 6, 2004

ABSTRACT: Novel carbazole-containing polymers, i.e., poly(3,6-di-*tert*-butyl-*N*-(*p*-ethynylphenyl)carbazole) [poly(*t*-Bu₂CzPA)] and poly(*N*-(*p*-ethynylbenzoyl)carbazole) [poly(CzCOPA)] were synthesized by the polymerization of the corresponding carbazole-containing acetylene monomers using [(norbornadiene)-RhCl]₂-Et₃N, WCl₆-*n*-Bu₄Sn, and WCl₄ catalysts. The UV-vis absorption band edge wavelengths of the polymers obtained by the polymerization with W catalysts were longer than those of the Rh-based polymers. The photoluminescence quantum yield of the W-based poly(*t*-Bu₂CzPA) was 55%, while that of the Rh-based one was as low as 3.6%. The photocurrent of poly(*t*-Bu₂CzPA) was 40–50 times higher than the dark current. Poly(*t*-Bu₂CzPA) in conjunction with iridium complexes exhibited electroluminescence (13–18 cd/m²).

Introduction

Carbazole is a well-known hole-transporting and electroluminescent unit. Polymers containing carbazole moieties in the main chain or side chain have attracted much attention because of their unique properties, which allow various photonic applications such as photoconductive, electroluminescent, and photorefractive materials.¹ Meanwhile, polyacetylene derivatives exhibit unique characteristics such as semiconductivity, high gas permeability, helix inversion, and nonlinear optical properties.² It is expected that incorporation of carbazole moieties into polyacetylene will lead to the development of novel functional polymers based on synergistic actions of carbazole and main chain conjugation.

Tang et al. synthesized several polyacetylenes carrying carbazole chromophores which show photoluminescence and photoconductivity.³ Advincula et al. also synthesized a series of carbazole-substituted poly(phenylacetylene)s and examined the cross-linking reaction by electrochemical oxidation.⁴ The redox potential decreases with increasing length of the alkyl chain. Tabata et al. synthesized several poly(*N*-alkyl-3-ethynylcarbazole) derivatives to find that the resulting polymers take a pseudo-hexagonal columnar structure in the solid phase.⁵ We previously synthesized poly(*N*-carbazolylacetylene), which shows a third-order susceptibility of 18×10^{-12} esu, two orders larger than that of poly(phenylacetylene).⁶ We also synthesized poly(3-(*N*-carbazolyl)-1-propyne), but the polymer obtained is insoluble in any solvents.⁷ On the other hand, poly(1-(*p*-*N*-carbazolylphenyl)-2-phenylacetylene) is partly soluble in toluene and chloroform and the polymer film shows photoconductivity and redox activity.⁸ More recently, we synthesized poly(9-(4-ethynylphenyl)carbazole) [poly(*p*-CzPA)] with Rh and W catalysts.⁹ Poly(*p*-CzPA) ob-



tained by WCl₆-*n*-Bu₄Sn-catalyzed polymerization exhibited UV-vis absorption apparently at a longer wavelength than the MoCl₅-*n*-Bu₄Sn-based counterpart did. Poly(*p*-CzPA) is expected to show unique properties based on the conjugated structure of polyacetylene main chain and carbazolylphenyl side chain. Unfortunately, however, poly(*p*-CzPA) is poorly soluble in organic solvents and the strength of the film is insufficient to elucidate the photo- and electroluminescence properties.

This article deals with the synthesis of novel solvent-soluble poly(*p*-CzPA) derivatives, poly(3,6-di-*tert*-butyl-*N*-(*p*-ethynylphenyl)carbazole) [poly(*t*-Bu₂CzPA)] and poly(*N*-(*p*-ethynylbenzoyl)carbazole) [poly(CzCOPA)] (Scheme 1), and characterization of the polymers to obtain information on their possibility as photo- and electroluminescence materials.

Experimental Section

Measurements. ¹H (400 MHz) and ¹³C (100 MHz) NMR spectra were recorded on a JEOL EX-400 spectrometer using tetramethylsilane as an internal standard. IR, UV-vis, and fluorescence spectra were measured on Shimadzu FTIR-8100, JASCO V-550, and JASCO FP750 spectrophotometers, respectively. Melting points (mp) were measured by a Yanaco micro melting point apparatus. Elemental analysis was carried out at the Kyoto University Elemental Analysis Center. The number- and weight-average molecular weights (*M_n* and *M_w*) of polymers were determined by gel permeation chromatog-

* Corresponding authors. Phone: +81-75-383-2589. Fax: +81-75-383-2590. E-mail: sanda@adv.polym.kyoto-u.ac.jp and masuda@adv.polym.kyoto-u.ac.jp.

[†] Kyoto University.

[‡] Chiba University.

raphy (GPC) on a JASCO GULLIVER system (PU-980, CO-965, RI-930, and UV-1570) equipped with polystyrene gel columns (Shodex columns K804, K805, and J806) using tetrahydrofuran (THF) as an eluent at a flow rate of 1.0 mL/min, calibrated by polystyrene standards at 40 °C. Thermal gravimetric analysis (TGA) was carried out with a Perkin-Elmer TGA-7.

Evaluation of Photoconductivity. A 2 wt % solution of poly(*t*-Bu₂CzPA) in THF was cast on an ITO electrode and then dried for 6 h in vacuo to prepare a thin film with a thickness of 2 μm. Au was vacuum-evaporated to prepare a counter electrode for the ITO electrode. The relationships between current (*I*) and applied voltage (*V*) for the ITO/poly(*t*-Bu₂CzPA) film/Au cells (effective electrode area 0.24 cm²) were measured at room temperature under reduced pressure of 10⁻² Torr in the dark and under photoillumination (2.5 mW/m²) with a Xe lamp using a thermoabsorption filter. Mobility was measured by conventional time-of-flight (TOF) techniques. The cell was placed in a cryostat, and the pressure was reduced below ca. 10⁻² Torr. A N₂ gas laser (NDC JS-1000L, 337 nm pulse, pulse duration of 5 ns, max light intensity of 5 mJ) was irradiated on a positively biased ITO electrode. The transient photocurrent signal was monitored using a digital storage oscilloscope (Tektronix TDS3012).

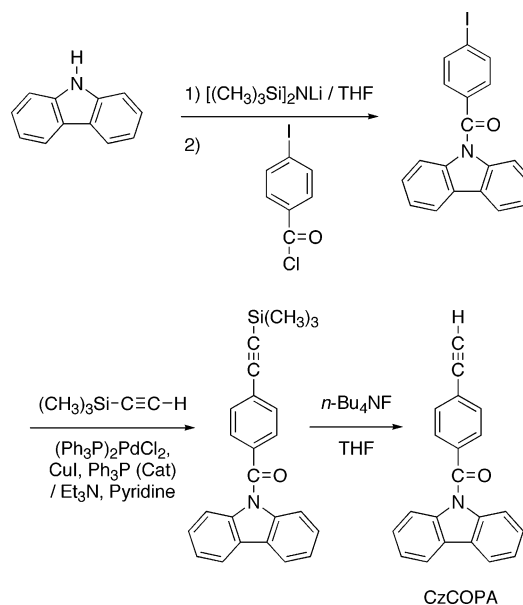
Evaluation of Electroluminescence. On a glass substrate with a patterned ITO electrode, a hole buffer layer of poly(ethylenedioxythiophene)/polystyrenesulfonic acid (PEDOT/PSS) was formed by spin-coating method, and subsequently a light-emitting layer was formed by spin-coating a solution of poly(*t*-Bu₂CzPA), 2-(4-*tert*-butylphenyl)-5-(4-biphenyl)-1,3,4-oxadiazole (PBD), and an Ir complex (weight ratio 60:32:8) in toluene. The thicknesses of each layer were 80 nm. Then 20-nm-thick calcium and 150-nm-thick aluminum as a cathode were deposited by high-vacuum thermal evaporation, and current density–voltage–luminance characteristics were measured.

Materials. Unless otherwise stated, reagents were commercially obtained and used without further purification. 3,6-Di-*tert*-butyl-*N*-(*p*-ethynylphenyl)carbazole was synthesized according to the literature.¹⁰ The solvents for polymerization were purified before use by the standard methods. Iridium(III) tris(2-(4'-*tert*-butylphenyl)pyridinato),¹¹ [Ir(*t*-Buppy)₃], and iridium(III) bis(2-(2'-benzothienyl)pyridinato-*N*,*C*^{3'})(acetylacetonate),¹² [Ir(btp)₂(acac)], were prepared according to the literature. PBD and PEDOT/PSS (Baytron P CH8000) were purchased from Dojindo Molecular Technologies, Inc. and H. C. Starck–V TECH Ltd., respectively.

***N*-(*p*-Iodobenzoyl)carbazole.** A solution of lithium bis(trimethylsilyl)amide in THF (29%, 33 mL, 56 mmol) was added to a solution of carbazole (9.3 g, 56 mmol) in THF (120 mL) at -78 °C. The reaction mixture was warmed to room temperature and stirred for 2 h. It was again cooled to -78 °C, and a solution of *p*-iodobenzoyl chloride (15 g, 56 mmol) in THF (30 mL) was added to the mixture. The resulting mixture was stirred at that temperature for 1 h, and then it was stirred at room temperature overnight. The solvent was distilled off by rotary evaporation, and 1 M HCl was added to the residue. The mixture was extracted with ethyl acetate, and the organic layer was washed with water and aq NaCl. It was dried over anhydrous MgSO₄, and the solvent was distilled off by rotary evaporation. The residual mass was purified by silica gel column chromatography eluted with *n*-hexane/ethyl acetate, followed by recrystallization. Yield 12.8 g (32 mmol, 58%). ¹³C NMR (δ, DMSO-*d*₆): 100.7, 115.5, 120.6, 123.8, 125.7, 127.2, 130.8, 134.9, 138.2, 138.6, 168.6 (C=O).

***N*-(*p*-Ethynylbenzoyl)carbazole (CzCOPA).** A mixture of *N*-(*p*-iodobenzoyl)carbazole (12.6 g, 31.7 mmol), (trimethylsilyl)acetylene (5.3 mL, 37.5 mmol), PdCl₂(PPh₃)₂ (665 mg, 0.95 mmol), PPh₃ (993 mg, 3.80 mmol), CuI (1.08 g, 5.70 mmol), Et₃N (150 mL), and pyridine (150 mL) was stirred at room temperature overnight. Et₃N and pyridine were removed from the reaction mixture by evaporation. Ether and ethyl acetate were added to the resulting mass, and insoluble solid was filtered off. The filtrate was washed with 1 M HCl and aq NaCl. The organic layer was dried with anhydrous Na₂SO₄

Scheme 2



and concentrated to obtain crude *N*-(*p*-trimethylsilylethynylbenzoyl)carbazole (10.4 g, 28.3 mmol, 89%). *n*-Bu₄NF (1.0 M in THF, 21 mL) was added to *N*-(*p*-trimethylsilylethynylbenzoyl)carbazole (8.6 g, 23.4 mmol) in THF (340 mL) at 0 °C, and the resulting mixture was stirred at that temperature for 5 min. HCl (1 M) was added to the mixture, and the resulting mixture was extracted with ether. The organic layer was washed with aq NaCl and water subsequently, dried over anhydrous Na₂SO₄, and concentrated by rotary evaporation to obtain solid. It was purified by silica gel column chromatography eluted with *n*-hexane/ethyl acetate = 40/1 (volume ratio) and recrystallization from ethyl acetate and benzene subsequently to obtain a white solid. Yield 1.6 g (5.4 mmol, 17%). Mp 178.0–179.8 °C. ¹H NMR (δ, DMSO-*d*₆): 4.50 (s, 1H, -C≡H), 7.38–7.40 (m, 6H, Ar), 7.67–7.74 (m, 4H, Ar), 8.20–8.21 (m, 2H, Ar). ¹³C NMR (δ, DMSO-*d*₆): 82.8, 84.0 (C≡CH), 115.5, 120.6, 123.9, 125.7, 125.8, 127.2, 129.2, 132.5, 135.6, 138.6 (Ph), 168.4 (C=O). IR (cm⁻¹, KBr): 3272 (C≡CH), 1674 (C=O), 1605, 1489, 1478, 1453, 1443, 1406, 1362, 1343, 1327, 1304, 1233, 1217, 1183, 1075, 949, 872, 845, 760, 750, 723, 710, 691, 648, 639, 629, 615, 590, 565, 531, and 421. Anal. Calcd for C₂₁H₁₃NO: C, 85.40; H, 4.44; N, 4.74. Found: C, 85.72; H, 4.50; N, 4.57.

Polymerization. All polymerizations were carried out in a glass tube equipped with a three-way stopcock under nitrogen. The polymerization mixture was poured into a large amount of methanol or ether to precipitate a polymer. It was separated from the supernatant by filtration and dried under reduced pressure.

Spectroscopic Data of the Polymers. Poly(*t*-Bu₂CzPA): ¹H NMR (400 MHz, δ in ppm, C₆D₆) 0.6–1.6 (18H, br, -CH₃), 5.8–8.2 (11H, br, Ar and CH=C<), 4.71 (1H, br s, -CH=C<), 7.02 (2H, br s, Ar), 7.40 (4H, br s, Ar). IR (KBr, cm⁻¹) 2961, 1509, 1364, 810. Poly(CzCOPA): ¹H NMR (400 MHz, δ in ppm, 1,4-dioxane) 6.4–8.2 (br). IR (KBr, cm⁻¹) 1676, 1445, 1327, 1302, 754, 723.

Molecular Mechanics (MM) Calculation. All calculations were carried out with Wavefunction, Inc., Spartan '04 Windows.

Results and Discussion

Monomer Synthesis. Scheme 2 illustrates the synthetic routes for the novel *N*-(*p*-ethynylbenzoyl)carbazole monomer, CzCOPA. It was synthesized by the reaction of *p*-iodobenzoyl chloride with carbazole anion prepared with lithium bis(trimethylsilyl)amide as a base, followed by Sonogashira coupling with (trimethylsilyl)acetylene

Table 1. Polymerization of *t*-Bu₂CzPA and CzCOPA^a

run	monomer	catalyst-cocatalyst	solvent	polymer				
				time (h)	yield ^b (%)	$M_n \times 10^{-3c}$	M_w/M_n^c	color
1	<i>t</i> -Bu ₂ CzPA	[(nbd)RhCl] ₂ -Et ₃ N	toluene	3	99	212	2.3	yellow
2	<i>t</i> -Bu ₂ CzPA	WCl ₆ - <i>n</i> -Bu ₄ Sn	toluene	24	94	3	2.3	brown
3	CzCOPA	[(nbd)RhCl] ₂ -Et ₃ N	toluene ^d	3	94	156	1.5	yellow-brown
4	CzCOPA	[(nbd)RhCl] ₂ -Et ₃ N	THF	3	100	240	1.7	yellow
5	CzCOPA	WCl ₆ - <i>n</i> -Bu ₄ Sn	toluene	24	13	23	1.4	red
6	CzCOPA	WCl ₆ - <i>n</i> -Bu ₄ Sn	anisole	24	33	10	1.8	red
7	CzCOPA	WCl ₆ - <i>n</i> -Bu ₄ Sn	1,4-dioxane	24	13	44	1.6	red
8	CzCOPA	WCl ₄	benzene/methyl acetate (1/1, v/v) ^d	24	10	5	1.6	orange

^a Polymerization conditions; [M]₀ = 0.2 M, [Rh] = 2.0 mM, [W] = 10 mM, [cocatalyst]/[catalyst] = 2.0, at 30 °C. ^b Methanol- or ether-insoluble part. ^c THF-soluble part, determined by GPC (THF, PSt). ^d [M]₀ = 0.1 M.

Table 2. Solubility of Poly(*t*-Bu₂CzPA) and Poly(CzCOPA)^a

polymer ^b	solvent							
	C ₆ H ₆	toluene	anisole	CHCl ₃	ether	THF	1,4-dioxane	MeOH
poly(<i>t</i> -Bu ₂ CzPA) (Rh)	+++	+++	+	+++	++	+++	+	-
poly(<i>t</i> -Bu ₂ CzPA) (W)	+++	++	+++	++	+++	+++	++	-
poly(CzCOPA) (Rh)	+	+	+++	+	-	++	+++	+
poly(CzCOPA) (W)	+	+	+++	+++	-	+++	+++	-

^a +++: soluble. ++: partly insoluble. +: partly soluble. -: insoluble. ^b Rh and W in parentheses mean the catalyst used in the polymerization to obtain the polymer.

and desilylation using *n*-Bu₄NF. The reaction of carbazole with the acyl chloride in the absence of lithium bis(trimethylsilyl)amide resulted in recovery of carbazole, presumably due to the low nucleophilicity of carbazole. The structure was confirmed by ¹H and ¹³C NMR, IR, and elemental analysis.

Polymerization. Table 1 summarizes the conditions and results of the polymerization of the carbazole-containing novel acetylene monomers, catalyzed by [(nbd)RhCl]₂-Et₃N, WCl₆-*n*-Bu₄Sn, and WCl₄ in toluene, THF, anisole, 1,4-dioxane, cyclohexane, and benzene/methyl acetate (1/1, v/v) at 30 °C for 3–24 h. In the first stage of the polymerization of CzCOPA in toluene, the reaction mixture became heterogeneous due to precipitation of the polymer formed (runs 3 and 5). Otherwise, the polymerization proceeded homogeneously. The corresponding polymers with M_n ranging from 3 000 to 240 000 were obtained in 10% quantitative yield. [(nbd)RhCl]₂-Et₃N, developed by Tabata et al.,¹³ gave polymers with higher M_n in higher yields than W catalysts did. In our previous paper,⁹ the Rh complex catalyst also afforded the polymer of the phenylacetylene monomer carrying carbazole (*p*-CzPA) in a higher yield than the W catalyst did. On the contrary, Rh catalysts cannot polymerize disubstituted acetylenes, although W catalysts can. The difference of activities between Rh and W catalysts should be based on the difference of polymerization mechanisms, i.e., Rh-catalyzed polymerization of acetylene monomers proceeds via an insertion mechanism, while a W-catalyzed one proceeds via a metathesis mechanism. Vohlidal et al.¹⁴ and we¹⁵ reported that use of oxygen-atom-containing solvents, especially 1,4-dioxane, is effective in phenylacetylene polymerization with W catalysts to obtain high-molecular-weight poly(phenylacetylene). In the polymerization of CzCOPA, employment of anisole (run 6) and 1,4-dioxane (run 7) was effective to increase the polymer yield and M_n compared to that of toluene (run 5). Benzene/methyl acetate mixed solvent was also examined in the polymerization with WCl₄, but this system was not operative to increase the polymer yield and M_n (run 8). The color of the polymers obtained by polymerization with the Rh catalyst was yellow-brown, while that with the W catalysts was red-brown. This

should be caused by the difference of main chain structures (cis and trans) and conjugated lengths between the polymers.

Table 2 summarizes the solubility of the polymers in several organic solvents. Poly(*t*-Bu₂CzPA) was soluble in most of the solvents, irrespective of the catalyst used in the polymerization. The solubility of poly(*t*-Bu₂CzPA) was apparently good compared to that of the previously reported corresponding polymer without the *tert*-butyl group, i.e., the polymer without *tert*-butyl groups obtained by the polymerization with W catalyst was soluble in benzene, toluene, CHCl₃, and THF, but the polymer obtained by polymerization with Rh catalyst was insoluble in these solvents, probably due to the difference of the cis–trans configuration of the polyacetylene main chains based on the catalysts used.⁹ Aggregation between the inter- and/or intramolecular chains or formation of a molecular assemble also may be the reason for this insolubility. On the other hand, poly(CzCOPA) was highly soluble in polar solvents such as anisole, THF, and 1,4-dioxane but was not in non-polar solvents such as benzene and toluene. The difference in solubility according to the catalysts used is not as large in the present polymers.

Polymer Structure. The polymer structures were examined by ¹H NMR and IR spectroscopies. It has been reported that Rh catalysts predominantly afford polyacetylenes with cis structure, while W catalysts afford trans-rich polyacetylenes.² Unfortunately, however, the ¹H NMR signals of poly(*t*-Bu₂CzPA) and poly(CzCOPA) appeared very broadly, and the signal assignable to the olefinic proton in the polyacetylene main chain coalesced with aromatic proton signals, which makes it impossible to determine the cis/trans ratio of the main chain. The IR spectra of the polymers obtained by the polymerization with Rh and W catalysts exhibited almost the same patterns. No absorption peaks of $\nu_{\text{C-H}}$ and $\nu_{\text{C=C}}$ were observed around 3270 and 2120 cm⁻¹, respectively, which confirms polymerization of the acetylene group. Otherwise, the IR spectroscopic patterns of the polymers were similar to those of the corresponding monomers.

Polymer Properties. Figure 1 depicts the UV–vis spectra of poly(*t*-Bu₂CzPA) and poly(CzCOPA). Both of the polymers exhibited absorption peaks at a longer

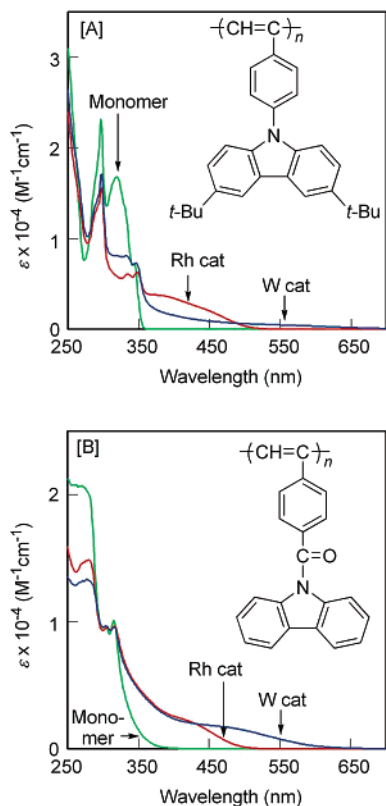


Figure 1. UV-vis spectra of (A) poly(*t*-Bu₂CzPA) and (B) poly(CzCOPA) obtained by the polymerization with Rh and W catalysts. The spectra of poly(*t*-Bu₂CzPA) and poly(CzCOPA) were measured in THF and 1,4-dioxane, respectively. Samples: runs 1, 2, 3, and 5 in Table 1.

wavelength than did the corresponding monomers, which is due to conjugation of the polyacetylene main chain. The polymers obtained by the W-catalyzed polymerization exhibited an UV-vis absorption band edge at a longer wavelength (640–700 nm) than the Rh-based ones (510–530 nm), which indicates the former polymers have a main chain conjugation longer than those of the latter.

Figure 2 shows fluorescence spectra of poly(*t*-Bu₂CzPA) obtained by the polymerization using Rh and W catalysts, along with photographs of the polymer solution emitting luminescence, whose maximum wavelength was observed at 410 nm upon excitation at 335 nm. It is noteworthy that the fluorescence quantum yield of the Rh-based polymer was only 3.6%, while that of the W-based one was as large as 55%. The monomers exhibited fluorescence at 370 nm when they were excited in a manner similar to the polymers. The polymers showed luminescence at wavelengths as much as 40 nm longer than the monomers.

Figure 3 shows the excitation spectrum of W-based poly(*t*-Bu₂CzPA) along with the UV-vis absorption spectra of poly(*t*-Bu₂CzPA) and the monomer. Both the absorption and excitation spectra of the polymer were red-shifted compared to the absorption spectrum of the monomer. It is likely that the excitation spectrum of poly(*t*-Bu₂CzPA) is not based on the interaction between the polyacetylene main chain and carbazole side chain but on an excimer formed between the carbazole side chains, because the spectroscopic pattern of the excitation spectrum was similar to that of carbazole. Figure 4 illustrates the molecular modeling of octamers of *t*-Bu₂CzPA having cis-trans and trans-trans main

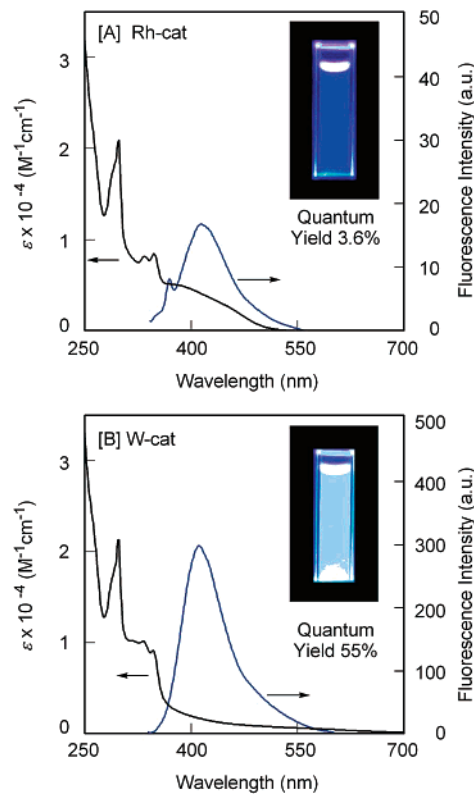


Figure 2. UV-vis and fluorescence spectra of poly(*t*-Bu₂CzPA) obtained by the polymerization with (A) Rh and (B) W catalysts measured in THF ($c = 5.3 \times 10^{-6}$ mol/L, excited at 335 nm). The photographs are the appearance of the sample solutions. Samples: runs 1 and 2 in Table 1.

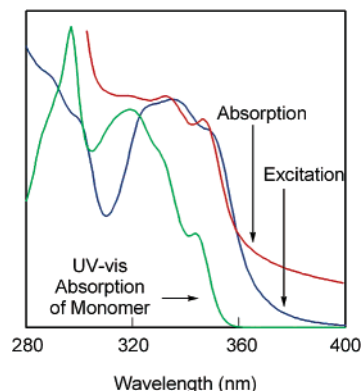


Figure 3. Absorption and excitation (emission 411 nm) spectra of W-based poly(*t*-Bu₂CzPA) measured in THF.

chains, which were optimized by molecular mechanics calculation. In the cis-trans geometry, the length between the carbazole side chains ranged from 4.5 to 4.7 Å. Meanwhile, in the trans-trans structure, it ranged from 5.0 to 5.5 Å. Although the main chain structures of the polymers in the present work are not clear, one can assume that cis-trans-rich and trans-trans-rich poly(*t*-Bu₂CzPA) were obtained by the polymerization with Rh and W catalysts, respectively.² It is therefore reasonable that W-based poly(*t*-Bu₂CzPA) exhibited large photoluminescence presumably based on the excimer of the side chain carbazoles, because the distance between the carbazole side chains is short enough, as demonstrated by molecular modeling. The trans-trans structure is apparently more sterically unfavorable than the cis-trans one. It therefore seems that the lower molecular weights of the W-based poly-

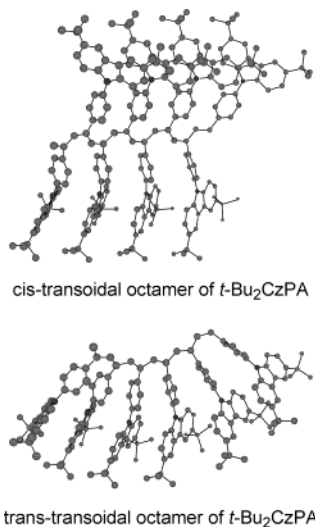


Figure 4. Geometries of cis–trans and trans–trans octamers of *t*-Bu₂CzPA optimized by MM. Hydrogen atoms are omitted for simplification.

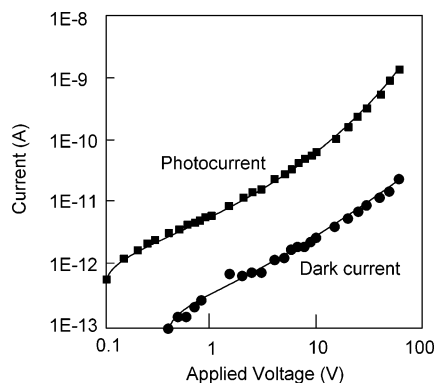


Figure 5. Relationships between current and voltage applied to ITO/poly(*t*-Bu₂CzPA)/Au cells (effective electrode area 0.24 cm², thickness 2 μm) measured at room temperature under reduced pressure of 10⁻² Torr. (●) Without photoirradiation. (■) Under photoirradiation (2.5 mW/m²) with a Xe lamp using a thermoabsorption filter. Polymer sample: run 1 in Table 1.

mers than those of the Rh-based ones are due to the steric factors.

Figure 5 depicts the I–V curve of an ITO/poly(*t*-Bu₂CzPA)/Au cell. The current was 40–50 times higher under photoillumination than without. This proves that poly(*t*-Bu₂CzPA) exhibits photoconductivity. The dark conductivity of poly(*t*-Bu₂CzPA) was calculated to be ca. 3×10^{-16} S/cm under an electric field of 10⁴–10⁵ V/cm. This value is 1 order higher than that of poly(vinylcarbazole) (PVCz),¹⁶ presumably due to π -conjugation of the poly(*t*-Bu₂CzPA) main chain. It has been reported that the photocurrent/dark current ratio of PVCz is less than 100.¹⁷ This value depends on several factors, including light intensity, illumination wavelength, and electric field. It is impossible to directly compare the photoconductivity of poly(*t*-Bu₂CzPA) with that of PVCz. However, the results in Figure 5 clearly indicate that the designed polymer works as an optoelectronic functional polymer. Figure 6 depicts double-logarithmic plots of the transient photocurrent of poly(*t*-Bu₂CzPA) under an electric field of 2.5×10^6 V/cm at room temperature. It should be noted that the transient signal of poly(*t*-Bu₂CzPA) represented dispersive character as seen in the inset (double linear plots) of Figure 6. This is due to the presence of multiple trapping levels in the poly(*t*-

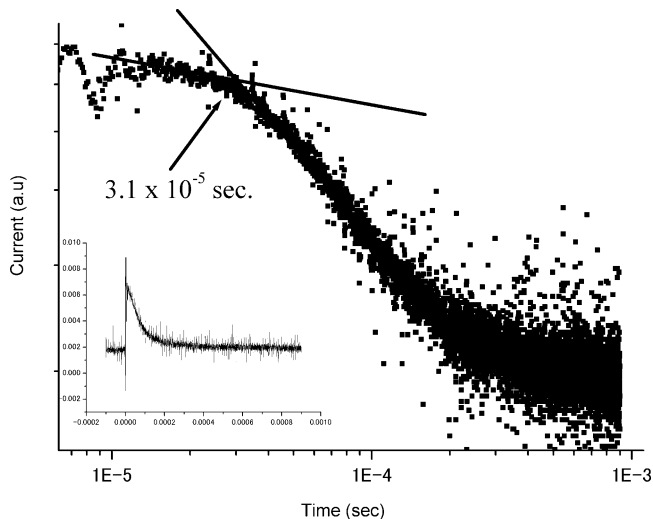


Figure 6. Double-logarithmic plots of the transient photocurrent of poly(*t*-Bu₂CzPA) under an electric field of 2.5×10^6 V/cm at room temperature. Polymer sample: run 1 in Table 1.

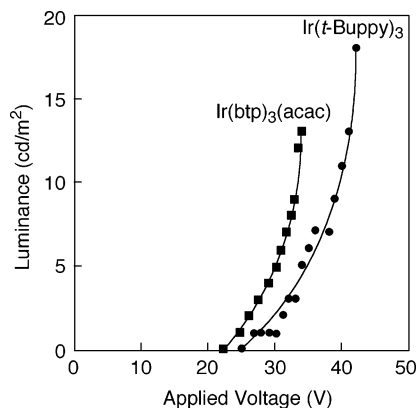


Figure 7. Relationships between luminance and voltage applied to poly(*t*-Bu₂CzPA) (60 wt %), PBD (32 wt %), Ir(btp)₃(acac), or Ir(*t*-Buppy)₃ (8 wt %). Polymer sample: run 1 in Table 1.

Bu₂CzPA) bulk. Transient time was, therefore, estimated from the intersection of the asymptotes to the plateau and tail of a $\log t - \log I$ of the transient signal as shown in Figure 6. The mobility was calculated to be ca. 3×10^{-6} cm²/V s. The mobility of PVCz has been reported to be ca. 10^{-6} cm²/V s under an electric field of 4×10^5 V/cm.¹⁸ Poly(*t*-Bu₂CzPA) showed lower mobility when the 1 order higher electric field of the present measurement was taken into account. Bulky *t*-Bu groups may work positively for solubility and processability but negatively for carrier transport by hindering the carrier transport pathways. On the other hand, the high conductivity in poly(*t*-Bu₂CzPA) in comparison with PVCz can be explained by the larger number of charge carriers. It is assumed that the electronic interaction between the π -conjugation system of the poly(*t*-Bu₂CzPA) main chain and that of the side chain carbazole group through the phenylene unit is effective for carrier generation but is not extended enough to stimulate charge carrier transport.

Figure 7 depicts the electroluminescence properties of poly(*t*-Bu₂CzPA) doped with Ir(btp)₃(acac) or Ir(*t*-Buppy)₃ using PBD as an electron-transporting agent. The device started emitting luminescence when 20–25 V was applied to the electrode. The luminance maxi-

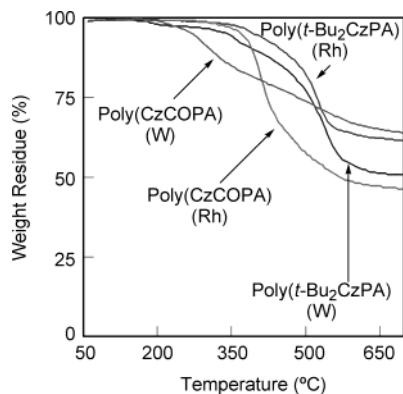


Figure 8. TGA curves of poly(*t*-Bu₂CzPA) and poly(CzCOPA) obtained by the polymerization with Rh and W catalysts measured in nitrogen with a heating rate of 10 °C/min.

lum was 13–18 cd/m². The electroluminescence efficiency was low compared to those of PVCz and poly(4-(9-carbazolylstyrene)).¹⁹ The lower electroluminescence efficiency of the carbazole-containing polyacetylene than the carbazole-containing vinyl polymers may be due to quenching of the luminescence of the Ir complexes by the polyacetylene main chain. The high light-emitting voltage of the device is possibly due to the lower charge carrier mobility of poly(*t*-Bu₂CzPA) than that of PVCz.

Figure 8 depicts the TGA traces of the polymers measured under nitrogen. The weight loss began around 200 °C and continued gradually up to 700 °C. In the early stage of the TGA measurement, the W-based polymers lost their weight faster than Rh-based polymers. Considering that the former polymers have a predominantly trans–trans structure, it seems that the main chain fission takes place more rapidly due to the steric repulsion between polymer side chains larger than the latter ones, as shown in Figure 4.

Summary

In this article we demonstrated the synthesis of novel carbazole-containing polyacetylenes, poly(*t*-Bu₂CzPA) and poly(CzCOPA). Both the polymers obtained by the polymerization using W catalysts exhibited UV–vis absorption band edges at longer wavelengths than the Rh-based ones. It seems that the W-based polymers have main chain conjugation longer than the Rh-based counterparts. Poly(*t*-Bu₂CzPA) showed conductivity 1 order higher than that of PVCz, probably due to the larger number of charge carriers. The current of poly(*t*-Bu₂CzPA) under photoirradiation was 40–50 times higher than that in the dark. It was confirmed that it works as an optoelectronic functional polymer. The electron mobility of poly(*t*-Bu₂CzPA) was lower than that of PVCz. The hindrance of carrier transport pathways by the bulky *t*-Bu group may be responsible for this result. Poly(*t*-Bu₂CzPA) doped with Ir(btp)₃(acac) or Ir(*t*-Buppy)₃ emitted luminescence when 20–25 V was applied.

Acknowledgment. The authors thank Professor Shinzaburo Ito and Dr. Hideo Ohkita at Kyoto Univer-

sity for their helpful discussion. The authors are grateful to Mr. Motoaki Kamachi at Showa Denko Co. for the measurement of the electroluminescence properties of the polymers.

References and Notes

- (1) For reviews, see: (a) Kippelen, B.; Gommé, A.; Hendrickx, E.; Wang, J. F.; Marder, S. R.; Peyghambarian, N. Photorefractive Polymers and Polymer-Dispersed Liquid Crystals. In *Field Responsive Polymers: Electroresponsive, Photoresponsive, and Responsive Polymers in Chemistry and Biology*; Khan, I. M., Harrison, J. S., Eds.; ACS Symposium Series 726; American Chemical Society: Washington, D.C., 1999; p 204. (b) Wang, Y. Z.; Epstein, A. *J. Acc. Chem. Res.* **1999**, *32*, 217. (c) Kippelen, B.; Meerholz, K.; Peyghambarian, N. An Introduction to Photorefractive Polymers. In *Nonlinear Optics of Organic Molecules and Polymers*; Nalwa, H. S., Miyata, S., Eds.; CRC: Boca Raton, FL, 1997; p 465.
- (2) For reviews, see: (a) Nagai, K.; Masuda, T.; Nakagawa, T.; Freeman, B. D.; Pinnau, I. *Prog. Polym. Sci.* **2001**, *26*, 721. (b) Masuda, T. Acetylenic Polymers. In *Polymeric Material Encyclopedia*; Salamone, J. C., Ed.; CRC Press: New York, 1996; Vol. 1, p 32.
- (3) (a) Xie, Z. L.; Lam, J. W. Y.; Qiu, C. F.; Wong, M.; Kwok, H. S.; Tang, B. Z. *Polym. Mater. Sci. Eng.* **2003**, *89*, 416. (b) Xie, Z. L.; Lam, J. W. Y.; Qiu, C. F.; Man, W.; Kwok, H. S.; Tang, B. Z. *Polym. Mater. Sci. Eng.* **2003**, *88*, 410. (c) Xie, Z. L.; Lam, J. W. Y.; Chen, J.; Dong, Y. P.; Qiu, C. F.; Man, W.; Kwok, H. S.; Tang, B. Z. *ACS Polym. Prepr.* **2002**, *43*(1), 411. (d) Lee, P. P. S.; Cheuk, K. K. L.; Dong, Y. P.; Chau, F. S. W.; Tang, B. Z. *Polym. Mater. Sci. Eng.* **2001**, *84*, 637. (e) Dong, Y. P.; Lam, J. W. Y.; Lee, P. P. S.; Tang, B. Z. *Polym. Mater. Sci. Eng.* **2001**, *84*, 616. (f) Lee, P. P. S.; Dong, Y. P.; Cheuk, K. K. L.; Chau, F. S. W.; Tang, B. Z. *ACS Polym. Prepr.* **2001**, *42*(1), 502. (g) Tang, B. Z.; Chen, H. Z.; Xu, R. S.; Lam, J. W. Y.; Cheuk, K. K. L.; Wong, H. N. C.; Wang, M. *Chem. Mater.* **2000**, *12*, 213. (h) Pui-Sze Lee, P.; Geng, Y.; Kwok, H. S.; Tang, B. Z. *Thin Solid Films* **2000**, *363*, 149.
- (4) Onishi, K.; Advincula, R. C.; Abdul Karim, S. M.; Nakai, T.; Masuda, T. *ACS Polym. Prepr.* **2002**, *43*(1), 171.
- (5) Fukushima, T.; Sone, T.; Tabata, M.; Sadahiro, Y. IUPAC World Polymer Congress 2002, Beijing, China, Preprints p 167.
- (6) Sata, T.; Nomura, R.; Wada, T.; Sasabe, H.; Masuda, T. *J. Polym. Sci., Part A: Polym. Chem.* **1998**, *36*, 2489.
- (7) Nakano, M.; Masuda, T.; Higashimura, T. *Polym. Bull.* **1995**, *34*, 191.
- (8) Tachimori, H.; Masuda, T. *J. Polym. Sci., Part A: Polym. Chem.* **1995**, *33*, 2079.
- (9) Sanda, F.; Kawaguchi, T.; Masuda, T.; Kobayashi, N. *Macromolecules* **2003**, *36*, 2224.
- (10) Zhu, Z.; Moore, J. S. *J. Org. Chem.* **2000**, *65*, 116.
- (11) Zhu, W.; Liu, C.; Su, L.; Yang, W.; Yuan, M.; Cao, Y. *J. Mater. Chem.* **2003**, *13*, 50.
- (12) Lamansky, S.; Djurovich, P.; Murphy, D.; Abdel-Razzaq, F.; Lee, H. E.; Adachi, C.; Burrows, P. E.; Forrest, S. R.; Thompson, M. E. *J. Am. Chem. Soc.* **2001**, *123*, 4304.
- (13) Tabata, M.; Yang, W.; Yokota, K. *Polym. J.* **1990**, *22*, 1105.
- (14) Sedlacek, J.; Pacovska, M.; Vohlidal, J.; Grubisic-Gallot, Z.; Zigon, M. *Macromol. Chem. Phys.* **1995**, *196*, 1705.
- (15) Masuda, T.; Takahashi, T.; Yamamoto, K.; Higashimura, T. *J. Polym. Sci., Polym. Chem. Ed.* **1982**, *20*, 2603.
- (16) Okamoto, K.; Kusabayashi, S.; Mikawa, H. *Bull. Chem. Soc. Jpn.* **1973**, *46*, 1953.
- (17) Okamoto, K.; Kusabayashi, S.; Mikawa, H. *Bull. Chem. Soc. Jpn.* **1973**, *46*, 2324.
- (18) Yoshida, M.; Ayano, M.; Kobayashi, N. *J. Polym. Sci., Part B: Polym. Phys.* **2000**, *38*, 362.
- (19) The devices similarly formulated from PVCz and poly(4-(9-carbazolylstyrene)) using Ir(*t*-Buppy)₃ as a dopant started emitting luminescence at 5–6 V, and the luminance maxima were 4020 and 6290 cd/m², respectively.

MA035972G